

## COMMUNICATIONS

<sup>13</sup>C Natural Abundance S<sup>3</sup>E and S<sup>3</sup>CT Experiments for Measurement of *J* Coupling Constants between <sup>13</sup>C<sup>α</sup> or <sup>1</sup>H<sup>α</sup> and Other Protons in a ProteinMorten Dahl Sørensen,<sup>1</sup> Axel Meissner, and Ole Winneche Sørensen

Department of Chemistry, Carlsberg Laboratory, Gamle Carlsberg Vej 10, DK-2500 Valby, Denmark

Received May 28, 1998; revised October 6, 1998

**It is demonstrated that the spin-state-selective pulse sequence elements, S<sup>3</sup>E and S<sup>3</sup>CT, previously introduced for measurement of *J* coupling constants in <sup>15</sup>N-labeled proteins can be applied for work with peptides and proteins with <sup>13</sup>C at the natural abundance level. In addition, a method is described for suppression of crosstalk caused by passive spin flips and pulse imperfections, which otherwise results in systematically underestimated *J* coupling constants and thereby inaccurate structural constraints. This method is also applicable for crosstalk suppression in applications of S<sup>3</sup>E and S<sup>3</sup>CT to <sup>13</sup>C- or <sup>15</sup>N-labeled samples. Experimental confirmation is obtained using a 10 mM BPTI sample focusing on <sup>13</sup>C in the α position. The measured *J* coupling constants include <sup>3</sup>*J*(H<sup>N</sup>-H<sup>α</sup>) and <sup>3</sup>*J*(H<sup>α</sup>-H<sup>β</sup>) related to the φ and χ<sup>1</sup> angles, respectively.** © 1999 Academic Press

**Key Words:** S<sup>3</sup>E; S<sup>3</sup>CT; E.COSY; *J* coupling constants; multidimensional NMR; crosstalk.

In <sup>13</sup>C, <sup>15</sup>N-labeled proteins a wide range of NMR pulse techniques exist for chemical shift correlations and measurement of *J* coupling constants. They are very efficient because typically all coherence transfers rely on one-bond coupling constants.

For unlabeled proteins these techniques cannot be employed, as it is realistic only to retrieve signals from molecules with a single <sup>13</sup>C or <sup>15</sup>N nucleus, and with current spectrometer sensitivity a relatively high concentration is required. Fortunately, only a single heterolabel is required for E.COSY-type (1–3) measurement of homo- and heteronuclear *J* coupling constants over more than one bond, provided homonuclear <sup>1</sup>H–<sup>1</sup>H coherence transfer is feasible (4, 5). The addition of spin-state-selective excitation (S<sup>3</sup>E) (6–9) or coherence transfer (S<sup>3</sup>CT) (10) to these techniques have resulted in convenient and accurate methods for extraction of interesting *J* coupling constants, as has been demonstrated for <sup>15</sup>N-labeled proteins.

It is the purpose of this Communication to adapt the two-

dimensional S<sup>3</sup>E and S<sup>3</sup>CT techniques to work with <sup>13</sup>C at the natural abundance level in peptides and proteins. For two main reasons we focus on molecules with the <sup>13</sup>C label at the α carbon. First of all, C<sup>α</sup> plays a pivotal role in the backbone of proteins as it is where the side chain is attached. Hence *J* coupling constants involving C<sup>α</sup> or H<sup>α</sup> represent crucial structural constraints. Secondly, measurement of *J* coupling constants between C<sup>α</sup> or the attached H<sup>α</sup> and other protons by S<sup>3</sup>E or S<sup>3</sup>CT 2D or 3D techniques require that other spectral areas than the one of H<sup>α</sup> be detected. That is of immense convenience considering that the water resonance is in the H<sup>α</sup> spectral region.

In Fig. 1 are shown four different pulse sequences that are relevant for the applications in mind. They represent the four combinations of either 2D homo- or heteronuclear correlation with measurement of either homo- or heteronuclear *J* coupling constants. S<sup>3</sup>E as well as S<sup>3</sup>CT could be employed in all four cases, but S<sup>3</sup>E for homonuclear and S<sup>3</sup>CT for heteronuclear correlation yield the respective shortest pulse sequences.

All these sequences have in common an element π/2 (water selective)–gradient–π/2 (nonselective) after the homonuclear coherence transfer (denoted *mixing* in the pulse sequences in Fig. 1) by, e.g., TOCSY or NOESY that ensures minimal water signal excitation. A relatively short water selective pulse can be employed, as it is immaterial if α proton signals are also eliminated. Alternatively, Watergate (11) could be considered instead of the π/2 (water selective)–gradient–π/2 (nonselective) element. Another common feature of the pulse sequences in Fig. 1 is the initial bilinear rotation that creates longitudinal two-spin order for protons attached to <sup>13</sup>C while other <sup>1</sup>H magnetizations are transverse and can be suppressed by a pulsed field gradient. The selective π/2 C<sup>α</sup> excitation pulse in the heteronuclear correlated sequences in Figs. 1a and 1b only serves to restrict the spectral range in *t*<sub>1</sub>. In other applications one could well imagine a nonselective pulse at this point in order to cover a larger number of carbon resonances.

The pulse sequence in Fig. 1a employs S<sup>3</sup>CT for coher-

<sup>1</sup> Current address: Department of Chemical Research, Leo Pharmaceutical Products, Industriparken 55, DK-2750 Ballerup, Denmark.

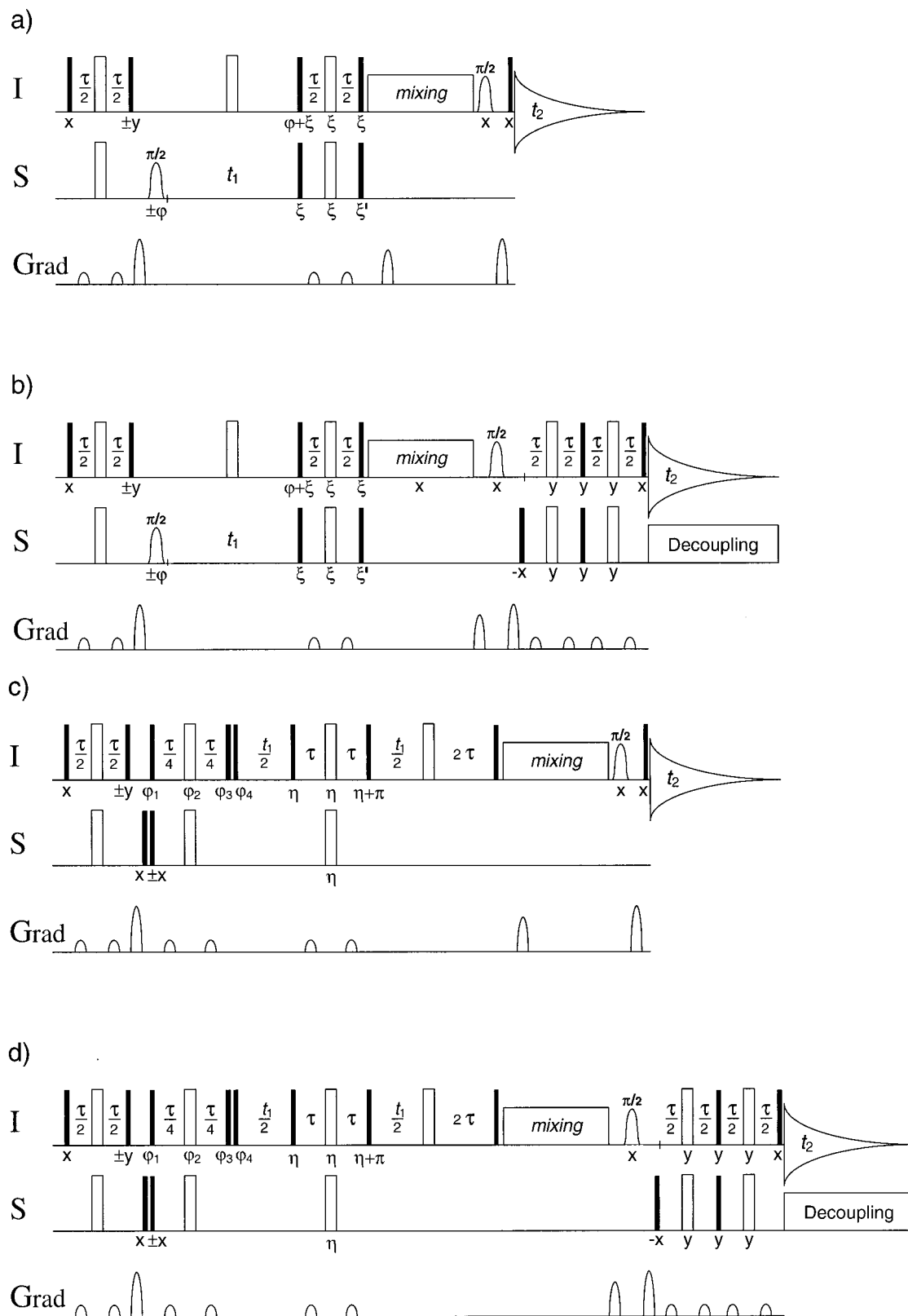


**FIG. 1.**  $S^3CT$  and  $S^3E$  pulse sequences for determination of homo- or heteronuclear  $J$  coupling constants. Filled and open bars represent  $\pi/2$  and  $\pi$  pulses, respectively. The shaped  $\pi/2$  I pulses are selective for the water signal and the shaped  $\pi/2$  S pulses are selective for the  $C^\alpha$  signals. The phases are indicated below the pulses (those with the prefix  $\pm$  indicate independent two-step phase cycles with relative receiver phase  $\pi$ ) and the delay  $\tau$  is  $(2J)^{-1}$ . The frame

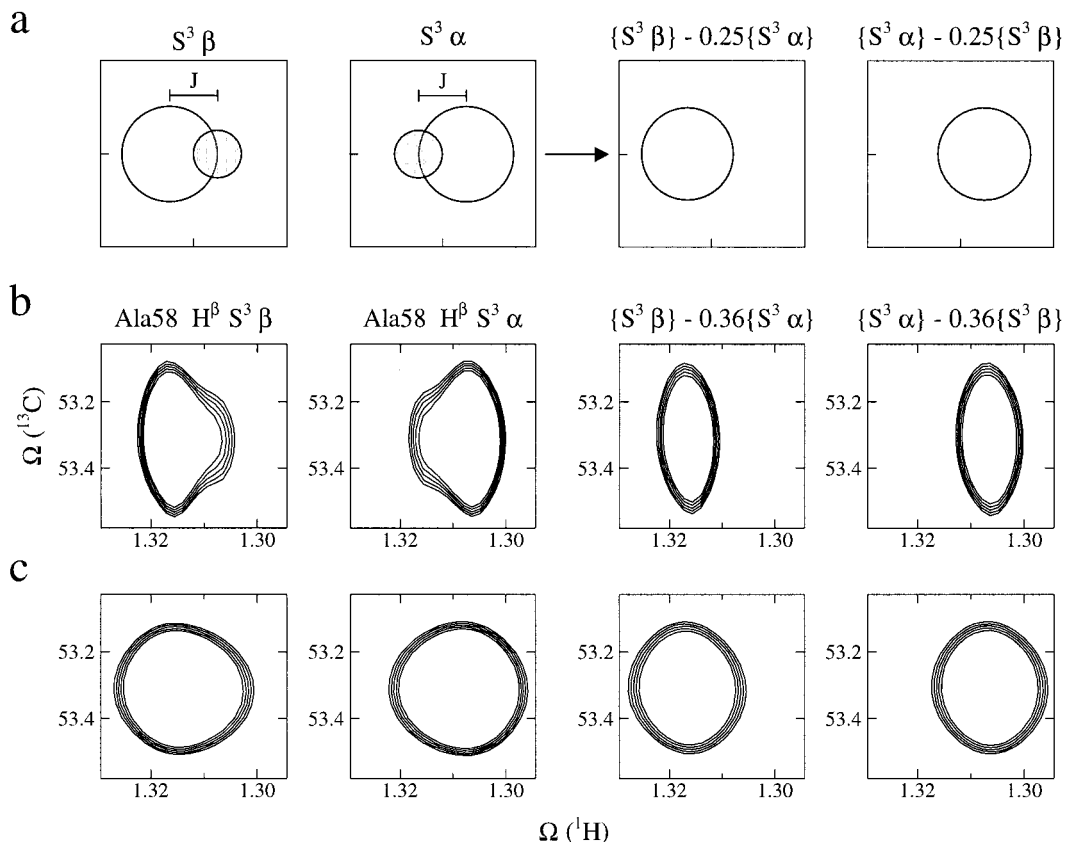


**FIG. 2.** (a) Schematic  $S^3CT$  or  $S^3E$  2D contour subspectra with 25% crosstalk indicated by the filled contour. The linear combinations  $\{S^3 \beta\} - 0.25\{S^3 \alpha\}$  and  $\{S^3 \alpha\} - 0.25\{S^3 \beta\}$  give clean subspectra without crosstalk. (b) Excerpt from a  $S^3CT$  TOCSY spectrum recorded with the sequence in Fig. 1b on a BPTI sample (details in Fig. 3 caption) showing the Ala58  $C^\alpha-H^\beta$  signal before and after compensating for crosstalk. The spectrum was processed as described in the legend to Fig. 3, except that a 5-Hz exponential line-broadening window function was used in  $t_2$ . The estimated Ala58  $H^\alpha-H^\beta$   $J$  coupling constants are 6.9 and 7.4 Hz before and after compensation for crosstalk, respectively. (c) Like (b), but processed with a 15 Hz exponential line-broadening window function in  $t_2$ . The estimated Ala58  $H^\alpha-H^\beta$   $J$  coupling constants are 5.2 and 7.4 Hz before and after compensation for crosstalk, respectively.

ence transfer from  $C^\alpha$  to  $H^\alpha$  and results in a  $^{13}C^\alpha-^1H$  correlation spectrum from which all heteronuclear  $J$  coupling constants from  $C^\alpha$  to protons can be measured. The only requirement is that  $^1H-^1H$  coherence transfer from  $H^\alpha$  to the respective protons be sufficiently efficient. This stipulation is critical for all the pulse sequences, and the preferred means of homonuclear coherence transfer are NOESY or TOCSY, although other techniques such as ROESY or relayed COSY could also serve. As described in detail else-

where (10),  $S^3CT$  excites in an intermediate state heteronuclear zero- and double-quantum coherence (ZQC and 2QC) which can be separated by a phase cycle or pulsed field gradients. Then follows a pulse-sequence element that is equivalent to a selective  $\pi$  rotation on, say, one of the two S-spin transitions. That rotation transfers the ZQC or 2QC exclusively to one of the two I-spin transitions.

The pulse sequence in Fig. 1b is the same as in Fig. 1a, but with a heteronuclear zero-quantum (ZQ)  $\pi$  rotation (5, 12–14)

designated *mixing* represents homonuclear coherence transfer by, e.g., isotropic TOCSY (e.g., by DIPSI-2 (21) or a delay for NOESY transfer. For NOESY, the phase cycling of Derome and Williamson (22) is employed. The phases and the editing scheme of the  $S^3CT$  E.COSY-type pulse sequences (a, b) are according to Sørensen *et al.* (10): The phase  $\varphi$  was cycled to create two data sets which contain both 2QC and ZQC: ( $\varphi = x, -x$  with receiver  $x, x$ ) and ( $\varphi = y, -y$  with receiver  $x, x$ ). Addition and subtraction, respectively, yield the edited subspectra.  $\xi' = \xi + \pi/2$ , where  $\xi$  is cycled in two steps ( $x, -x$ ) with relative receiver phase  $\pi$ . (a) Hetero-correlated  $S^3CT$  sequence for determination of heteronuclear  $J$  coupling constants; (b) hetero-correlated  $S^3CT$  sequence for determination of homonuclear  $J$  coupling constants. The phases and the editing scheme of the  $S^3E$  E.COSY-type pulse sequences (c, d) are according to Meissner *et al.* (6, 7): Two data sets with the phase vectors ( $\varphi_1, \varphi_2, \varphi_3, \varphi_4$ ) are recorded, i.e.,  $A: \{(\pi/4, 0, 0, 0) - (\pi/4, 0, \pi/2, \pi/2)\}$ ,  $B: \{(\pi/4, 0, 0, \pi) - (5\pi/4, 0, \pi/2, 3\pi/2)\}$ . The linear combinations  $A + B$  and  $A - B$  yield the edited subspectra with a relative phase shift of  $\pi/2$  in  $t_1$ . The phase  $\eta$  is cycled to select zero change in coherence order in a concerted manner, i.e., an  $n$ -step cycle with increments  $2\pi/n$ ,  $n \geq 3$ , at constant receiver phase. (c) Homo-correlated  $S^3E$  sequence for determination of heteronuclear  $J$  coupling constants; (d) homo-correlated  $S^3E$  sequence for determination of homonuclear  $J$  coupling constants.

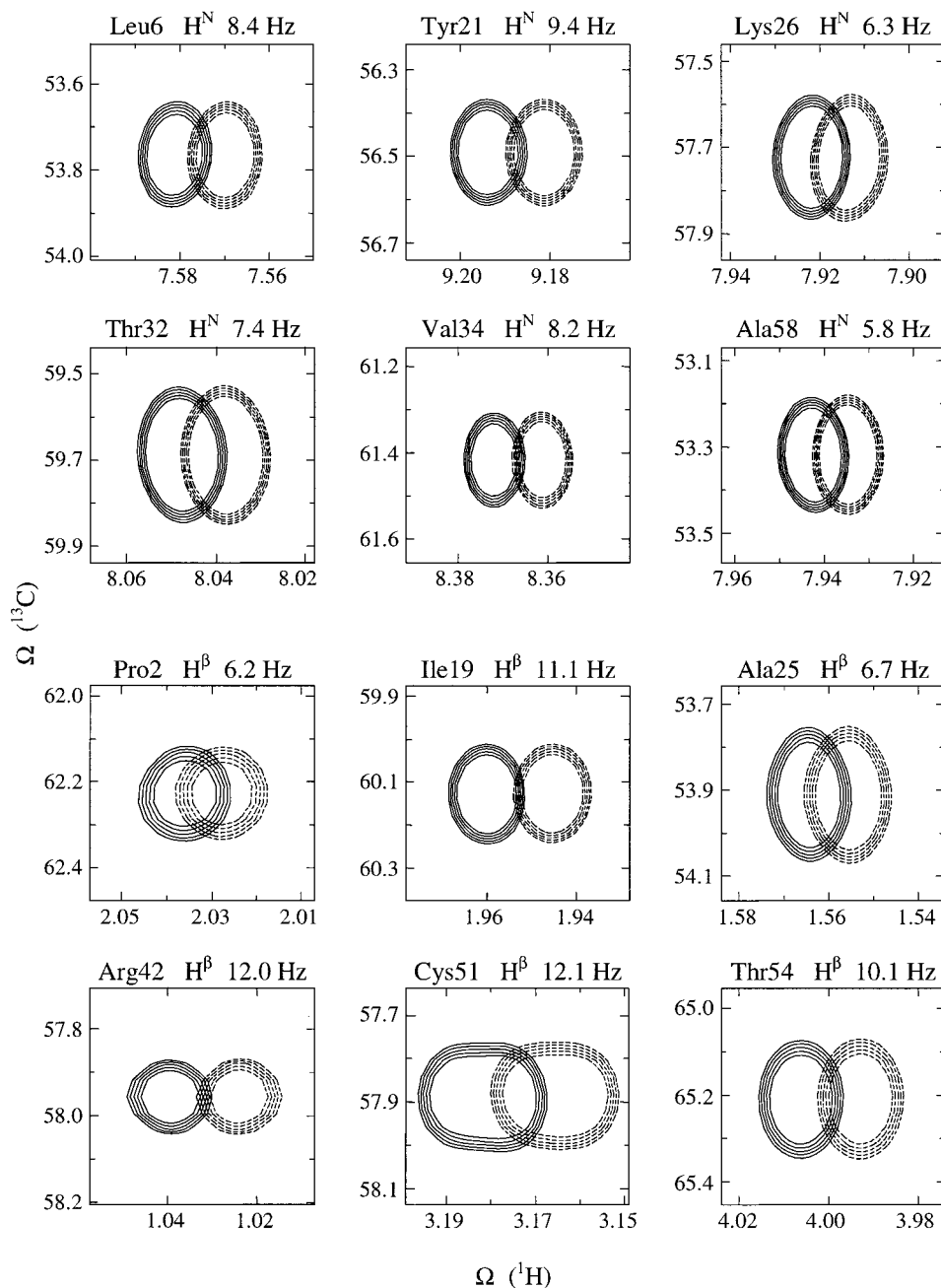


**FIG. 3.** Excerpts from a heteronuclear correlated  $S^3CT$  TOCSY spectrum of 10 mM BPTI (90%/10%  $H_2O/D_2O$ ) sample recorded with the sequence in Fig. 1b on a Varian Unity Inova 750 MHz spectrometer at 36°C. The spectrum was processed with the program XWINNMR 2.0 and the edited subspectra (solid and dashed lines) overlaid using the software package Pronto (21). The  $J$  coupling constants are homonuclear  $H^\alpha-H^N$  and  $H^\alpha-H^\beta$  coupling constants. Parameters: TOCSY mixing time 30 ms; solvent presaturation 1.5 s;  $\tau = 3.57$  ms; States-TPPI mode;  $t_1(\max)$  13.3 ms; 640 scans and 98 increments; exponential ( $lb = 15$  Hz) and squared  $\pi/2$  shifted sine-bell window functions in  $t_2$  and  $t_1$ , respectively. Spectral widths of 7400 and 9450 Hz were covered by a data matrix of  $196 \times 8192$  points zero-filled to  $1024 \times 8192$  points prior to Fourier transformation. The selective  $\pi/2$   $C^\alpha$  and  $\pi/2$  water pulses were a  $750 \mu s$  E-BURP (24) pulse and a 5.87 ms  $270^\circ$  Gauss pulse (25), respectively. The  $^{13}C$  and  $^1H$  carriers were positioned at 53.1 and 4.67 ppm, respectively. All signals were compensated for 28% crosstalk except Ala58  $C^\alpha-H^N$ , which was compensated for 36% crosstalk. The coupling constants were estimated from 1D sections with a precision of about 0.2 Hz. Alternatively, routines taking the entire 2D peak shapes into account are available within the program package PRONTO (<http://www.crc.dk>) (23).

appended at the end. That has the effect of converting the basic E.COSY-type cross peak multiplet patterns with  $C^\alpha$  in the role of the passive spin into patterns with  $H^\alpha$  in that role. Hence,

$J_{HH}$  coupling constants can be determined from 2D spectra recorded with this sequence (5).

The sequences in Figs. 1c and 1d correspond to those in

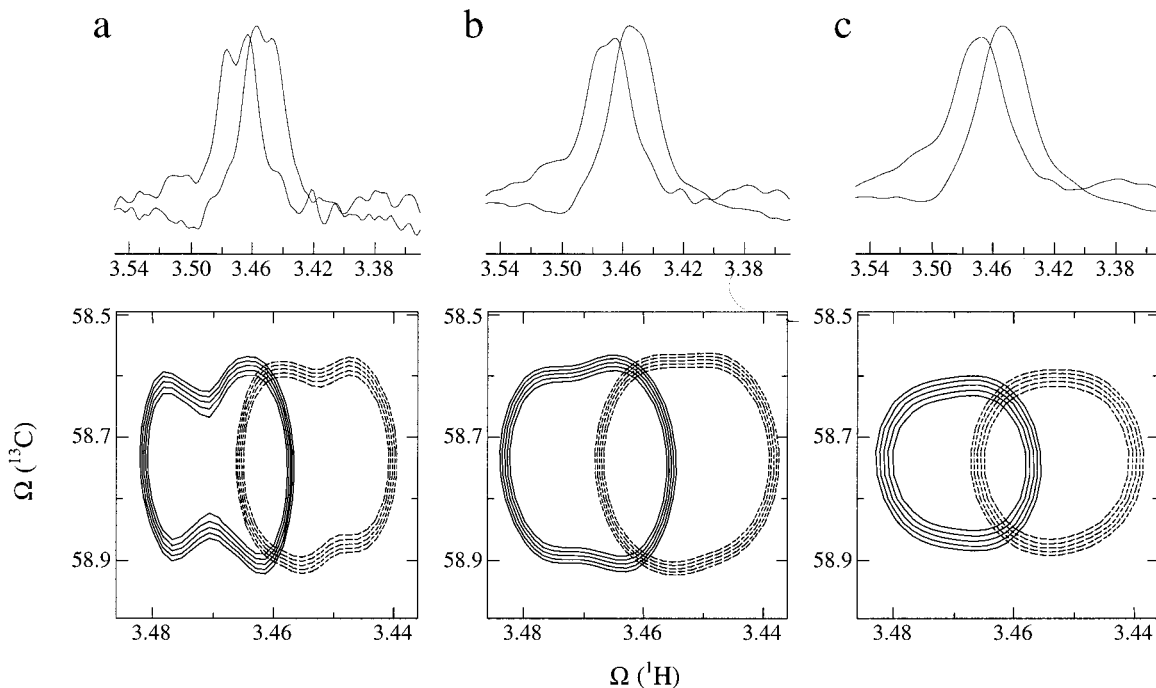


**FIG. 4.** Excerpts and traces from the  $S^3$ CT TOCSY spectrum of BPTI showing one of the Tyr23  $C^\alpha$ - $H^\beta$  signals. The spectrum was processed with (a) 5 Hz, (b) 10 Hz, and (c) 15 Hz line broadening, respectively, in the  $t_2$  dimension. The traces were taken at the Tyr23  $C^\alpha$  frequency. The estimated  $H^\alpha$ - $H^\beta$  coupling constant is 12.3 Hz.

Figs. 1a and 1b, respectively, but lead to homo- instead of heteronuclear 2D correlation spectra. They employ  $S^3$ E for editing into the two subspectra associated with the  $\alpha$  and  $\beta$  spin states, respectively, of either  $C^\alpha$  (Fig. 1c) or  $H^\alpha$  (Fig. 1d). Also included as an option for resolution and sensitivity enhancement is the BIRD element (15) in the middle of the evolution periods which provides homo- and heteronuclear decoupling in  $F_1$ .  $S^3$ E (6–9) is an alternative to  $S^3$ CT which is equivalent to a selective  $(\pi/2)_\varphi$  rotation on one of the transitions of a doublet followed by a nonselective  $\pi/2$  pulse on the same spin with phase  $\varphi + \pi/2$  in one experiment and  $\varphi - \pi/2$  in another. Addition and subtraction of these two data sets provides two subspectra corresponding to separate excitation of the two doublet components.

Both  $S^3$ E and  $S^3$ CT allow convenient measurements of  $J$  coupling constants by editing the spectrum into two subspectra according to the spin state of the passive spin. The  $J$  coupling constants are easily extracted from the relative peak displacements in the two subspectra. Nevertheless, there is a problem in both  $S^3$ E and  $S^3$ CT, as well as other E.COSY-type methods: namely, passive spins changing their state between two evolution periods of a multidimensional experiment (16–18). Passive spin flips lead to the appearance of additional components in the cross peak multiplets. That is, signals from systems where the passive spin in the first evolution period was in the  $\beta$  spin state will appear in the  $\alpha$  subspectrum and vice versa. Another source of crosstalk of this type is pulse imperfections.

As the linewidth in most proteins dominates the  $J$  coupling

constants of interest, the desired and undesired signals overlap and result in a single signal with maximum shifted in the direction of the undesired one. Accordingly, crosstalk due to passive spin flips results in an underestimation of the coupling constants when they are measured as separations of peaks. In the present work, crosstalk is suppressed by postprocessing of the edited subspectra (*vide infra*).

Figure 2a shows a schematic 2D  $S^3$ CT or  $S^3$ E spectrum where passive spin flip has led to 25% crosstalk. That is, the  $S^3 \beta$  ( $S^3 \alpha$ ) subspectrum consists of two signals with an intensity ratio of 1:0.25; one is the desired signal while the other is an undesired signal corresponding to the passive spin being in the  $\alpha$  ( $\beta$ ) spin state. The combinations  $\{S^3 \beta\} - 0.25\{S^3 \alpha\}$  and  $\{S^3 \alpha\} - 0.25\{S^3 \beta\}$  yield clean  $S^3 \beta$  and  $S^3 \alpha$  subspectra, respectively. Figures 2b and 2c show the Ala58  $C^\alpha$ - $H^\beta$  signals of an  $S^3$ CT spectrum recorded with the sequence in Fig. 1b on a sample of the protein bovine pancreatic trypsin inhibitor (BPTI) (19). It is immediately apparent from the subspectra processed with 5 Hz line broadening in  $t_2$  (Fig. 2b) that crosstalk is present due to Ala58  $C^\alpha/H^\alpha$  spin flips. Clean subspectra are in the case of Ala58 obtained by assuming 36% crosstalk when making the linear combinations (Fig. 2b). The crosstalk, although still visible, is not as evident when the spectra are processed with 15-Hz line broadening in  $t_2$  (Fig. 2c). The level of crosstalk may differ for different residues depending on local motion. Nevertheless, it was found that 28% compensation generally resulted in excellent suppression of crosstalk except for the C-terminal Ala58 requiring 36%.

This uniformity is handy when it comes to small  $J$  coupling constants because the required level of crosstalk compensation cannot be determined from the pertinent cross peaks.

Estimation of the level of crosstalk is easy in experiments for measurement of heteronuclear  $J$  coupling constants (Figs. 1a and 1c) because it can be done from the one-bond correlations with large doublet splitting. This is not the case in experiments for measurement of homonuclear coupling constants, and we currently rely on uniformity of crosstalk levels. In other words, the level of crosstalk for larger  $J$  coupling constants is estimated as shown in Fig. 2, and that same correction is then applied to other cross peaks. Notwithstanding, this approach cannot be applied to larger proteins and it is a subject of ongoing research to develop setup experiments for independent determination of the level of crosstalk. The complications from crosstalk apply both to enriched and natural-abundance samples. For quantification of errors from crosstalk in measured  $J$  coupling constants, we refer to Ref. (8).

Compensation for crosstalk in E.COSY-type spectra without application of  $S^3$ -based editing schemes could also be done by linear combinations as described above of a normal and a so-called complementary E.COSY spectrum (1–3). However, that would require separate recording of the complementary one, which would be detrimental to the overall sensitivity of the experiment.

Figure 3 shows excerpts from the BPTI  $S^3$ CT spectrum recorded with the sequence in Fig. 1b employing TOCSY for homonuclear mixing. The homonuclear three-bond  $H^\alpha-H^N$  and  $H^\alpha-H^\beta$   $J$  coupling constants which contain information about the  $\varphi$  and  $\chi^1$  angles, respectively, are easily extracted from the relative peak displacements in the subspectra compensated for crosstalk. The obtained coupling constants are in good agreement with those used in the determination of the BPTI structure (26). Small  $J_{HH}$  coupling constants are best extracted from a corresponding spectrum employing in this case more efficient NOESY transfer.

Determination of the  $H^\alpha-H^\beta$   $J$  coupling constants in  $C^\alpha H-C^\beta H_2$  systems is impeded by the fact that relaxation effects during detection introduces nonidentical submultiplet patterns for the two spin states of the passive spin (20). The asymmetric lineshape of the Tyr23  $C^\alpha-H^\beta$  multiplet in Fig. 4a illustrates these relaxation effects. The different shapes of the two submultiplets complicate determination of the coupling constant by fitting of the submultiplets. Extensive line broadening in the  $t_2$  dimension can, as shown in Figs. 4b and 4c, circumvent this problem as the fine structure is irrelevant for measurement of the interesting  $J$  values.

In conclusion, we have demonstrated the application of the pulse sequence elements  $S^3$ CT and  $S^3$ E for measurement of  $J$  coupling constants in peptides and proteins with  $^{13}C$  at the natural abundance level. Furthermore, it has been shown that crosstalk due to passive spin flips can be eliminated by post-processing of  $S^3$ -edited subspectra, which improves the accuracy of the measured  $J$  coupling constants.

## ACKNOWLEDGMENTS

The spectra presented have been recorded on the 750 MHz Varian Unity Inova spectrometer of the Danish Instrument Center for NMR Spectroscopy of Biological Macromolecules at Carlsberg Laboratory. We thank Poul Erik Hansen and Novo Nordisk A/S for the loan of the BPTI sample and Kurt D. Berndt for a list of the coupling constants used in the determination of the BPTI structure. A.M. is supported by a postdoctoral fellowship from the Deutsche Forschungsgemeinschaft.

## REFERENCES

1. C. Griesinger, O. W. Sørensen, and R. R. Ernst, *J. Am. Chem. Soc.* **107**, 6394–6395 (1985).
2. C. Griesinger, O. W. Sørensen, and R. R. Ernst, *J. Chem. Phys.* **85**, 6837–6852 (1986).
3. C. Griesinger, O. W. Sørensen, and R. R. Ernst, *J. Magn. Reson.* **75**, 474–492 (1987).
4. G. T. Montellione, M. E. Winkler, P. Rauenbühler, and G. Wagner, *J. Magn. Reson.* **82**, 198–204 (1989).
5. W. Willker, and D. Leibfritz, *J. Magn. Reson.* **99**, 421–425 (1992).
6. A. Meissner, J. Ø. Duus, and O. W. Sørensen, *J. Magn. Reson.* **128**, 92–97 (1997).
7. A. Meissner, J. Ø. Duus, and O. W. Sørensen, *J. Biomol. NMR* **10**, 89–94 (1997).
8. A. Meissner, T. Schulte-Herbrüggen, and O. W. Sørensen, *J. Am. Chem. Soc.* **120**, 7989–7990 (1998).
9. A. Meissner, T. Schulte-Herbrüggen, and O. W. Sørensen, *J. Am. Chem. Soc.* **120**, 3803–3804 (1998).
10. M. D. Sørensen, A. Meissner, and O. W. Sørensen, *J. Biomol. NMR* **10**, 181–186 (1997).
11. M. Piotto, V. Saudek, and V. Sklenar, *J. Biomol. NMR* **2**, 661–665 (1992).
12. J. Cavanagh, A. G. Palmer, P. E. Wright, and M. Rance, *J. Magn. Reson.* **91**, 429–436 (1991).
13. T. Schulte-Herbrüggen, Z. L. Mädi, O. W. Sørensen, and R. R. Ernst, *Mol. Phys.* **72**, 847–871 (1991).
14. L. E. Kay, P. Keifer, and T. Saarinen, *J. Am. Chem. Soc.* **114**, 10663–10665 (1992).
15. J. R. Garbow, D. P. Weitekamp, and A. Pines, *Chem. Phys. Lett.* **93**, 504–509 (1982).
16. G. T. Montellione, S. D. Emerson, and B. A. Lyons, *Biopolymers*, 327–334 (1992).
17. M. Görlach, M. Wittekind, B. T. Farmer II, L. E. Kay, and L. Mueller, *J. Magn. Reson. B* **101**, 194–197 (1993).
18. A. C. Wang, and A. Bax, *J. Am. Chem. Soc.* **118**, 2483–2494 (1996).
19. K. D. Berndt, P. Güntert, L. P. M. Orbons, and K. Wüthrich, *J. Mol. Biol.* **227**, 757–775 (1992).
20. D. P. Zimmer, J. P. Marino, and C. Griesinger, *Magn. Reson. Chem.* **34**, S177–S186 (1996).
21. A. J. Shaka, C. J. Lee, and A. Pines, *J. Magn. Reson.* **77**, 509–517 (1988).
22. A. E. Derome, and M. P. Williamson, *J. Magn. Reson.* **88**, 177–185 (1990).
23. M. Kjær, K. V. Andersen, and F. M. Poulsen, *Meth. Enzym.* **239**, 288–307 (1994).
24. H. Geen, and R. Freeman, *J. Magn. Reson.* **93**, 93–141 (1991).
25. L. Emsley, and G. Bodenhausen, *J. Magn. Reson.* **82**, 211–221 (1989).
26. K. D. Berndt, personal communication.